A conserved genetic interaction between Spt6 and Set2 regulates H3K36 methylation

Rajaraman Gopalakrishnan[1], Sharon K. Marr[2], Robert E. Kingston[1,2] and Fred Winston[1,*]

[1]Department of Genetics, Harvard Medical School, Boston, MA, USA 02115 and [2]Department of Molecular Biology, Massachusetts General Hospital, Boston, MA 02114, USA

ABSTRACT

The transcription elongation factor Spt6 and the H3K36 methyltransferase Set2 are both required for H3K36 methylation and transcriptional fidelity in *Saccharomyces cerevisiae*. However, the nature of the requirement for Spt6 has remained elusive. By selecting for suppressors of a transcriptional defect in an *spt6* mutant, we have isolated several highly clustered, dominant *SET2* mutations (*SET2*[sup] mutations) in a region encoding a proposed autoinhibitory domain. *SET2*[sup] mutations suppress the H3K36 methylation defect in the *spt6* mutant, as well as in other mutants that impair H3K36 methylation. We also show that *SET2*[sup] mutations overcome the requirement for certain Set2 domains for H3K36 methylation. *In vivo*, *SET2*[sup] mutants have elevated levels of H3K36 methylation and the purified Set2[sup] mutant protein has greater enzymatic activity *in vitro*. ChIP-seq studies demonstrate that the H3K36 methylation defect in the *spt6* mutant, as well as its suppression by a *SET2*[sup] mutation, occurs at a step following the recruitment of Set2 to chromatin. Other experiments show that a similar genetic relationship between Spt6 and Set2 exists in *Schizosaccharomyces pombe*. Taken together, our results suggest a conserved mechanism by which the Set2 autoinhibitory domain requires multiple Set2 interactions to ensure that H3K36 methylation occurs specifically on actively transcribed chromatin.

INTRODUCTION

The histone chaperone Spt6 is a highly conserved transcription elongation factor required for many aspects of transcription and chromatin structure. Spt6 binds directly to Rpb1, the largest subunit of RNA polymerase II (RNAPII) (1–6), to histones and nucleosomes (7–9), and to the essential transcription factor Spn1/Iws1 (9–12). Mutations in *Saccharomyces cerevisiae SPT6* cause genome-wide changes in histone occupancy (13–16) and impair several histone modifications, including H3K36 di- and tri-methylation (H3K36me2/me3) catalyzed by the H3K36 methyltransferase Set2 (17–20). Mutations in *SPT6* also cause greatly elevated levels of transcripts that arise from within coding regions on both sense and antisense strands, known as intragenic transcription (15,21–25). Intragenic transcription has recently emerged as a mechanism to express alternative genetic information within a coding region (for example, (26–30)).

Regulation of intragenic transcription by Spt6 occurs, at least in part, by its regulation of H3K36 methylation, as a deletion of *SET2* also causes genome-wide expression of intragenic transcripts (17,31,32). Set2 normally represses intragenic transcription via its association with RNAPII during transcription elongation, resulting in H3K36me2/me3 over gene bodies (33–36). This histone modification is required for the co-transcriptional function of the Rpd3S histone deacetylase complex (17,37–40). Deacetylation by Rpd3S over transcribed regions is believed to maintain a repressive environment that prevents intragenic transcription. Regulation of intragenic transcription by H3K36 methylation is conserved as depletion of *SETD2* (a human ortholog of yeast *SET2*) also results in the genome-wide expression of intragenic transcripts (41).

Set2-dependent H3K36me2/me3 is regulated by several factors in addition to Spt6. These include members of the PAF complex (33,42), as well as the Rpb1 CTD kinases Ctk1 (33,43) and Bur1 (18,42). Furthermore, there is strong evidence that a nucleosomal surface composed of specific residues of histones H2A, H3 and H4 near the entry and exit point of nucleosomal DNA forms a substrate recognition surface for Set2 (44,45). The H3 N-terminal tail itself has also been shown to be required for Set2 activity and mutant analysis suggests that intra-tail interactions (46) and *cis–trans* isomerization of the N-terminal H3 tail (47) control Set2 activity. The combined influence of all of these factors shows that Set2 activity is highly regulated to ensure that it occurs co-transcriptionally on a chromatin template.

Multiple domains within Set2 regulate its catalytic activity in order to ensure that it functions during transcription elongation. The C-terminal region of Set2 contains

*To whom correspondence should be addressed. Tel: +617 432 7768; Email: winston@genetics.med.harvard.edu

the Set2–Rpb1 interacting domain (SRI domain), which interacts with the Ser2- and Ser5-phosphorylated carboxy-terminal domain (CTD) of Rpb1 (48) and which binds nucleosomal DNA (49). A deletion of the SRI domain causes loss of H3K36 methylation (19). In addition, a nine amino acid sequence in the N-terminal region of Set2 mediates the interaction of Set2 with histone H4 and this domain is also required for Set2 catalytic activity (45). The central region of Set2 has been characterized as an autoinhibitory domain, as deletions throughout this region result in increased H3K36 methylation (49). However, the functional role of this domain is unknown.

The initial goal of our study was to identify factors that regulate Spt6-mediated intragenic transcription. To do this, we carried out a selection for suppressor mutations that inhibit intragenic transcription in an *spt6* mutant, where intragenic transcripts are widespread (22,23,25). We identified 20 independent, dominant mutations in *SET2* (*SET2^sup^* mutations) that encode a cluster of amino acid changes in the Set2 autoinhibitory domain. The isolation of these mutants led us to study the function of the autoinhibitory domain *in vivo*. Our results show that *SET2^sup^* mutations suppress H3K36me2/me3 defects in *spt6* and other transcription elongation factor mutants, as well as in *set2* mutants that normally abolish Set2 activity. In addition, we show that the loss of H3K36me2/me3 in *spt6-1004* and its suppression by the *SET2^sup^* mutations both occur genome-wide, primarily at a step beyond Set2 recruitment. Finally, we show that orthologous *SET2^sup^* mutations in *Schizosaccharomyces pombe* also partially rescue the H3K36 methylation defect in an *S. pombe spt6* mutant. Taken together, our results have revealed new insights into the regulation of Set2 and suggest that the autoinhibitory domain monitors multiple Set2 interactions that are required for its function *in vivo*.

MATERIALS AND METHODS

Yeast strains and media

All *S. cerevisiae* and *S. pombe* strains used in this study were constructed by standard methods and are listed in Supplementary Table S1. The *S. pombe set2Δ3* mutation was made based on alignment of the *S. cerevisiae* and *S. pombe* Set2 amino acid sequence using the Uniprot 'Align' tool (https://www.uniprot.org/help/sequence-alignments). All *S. cerevisiae* liquid cultures were grown in YPD (1% yeast extract, 2% peptone and 2% glucose) at 30°C unless mentioned otherwise. All *S. pombe* liquid cultures were grown in YES (0.5% yeast extract, 3% glucose, 225 mg/l each of adenine, histidine, leucine, uracil and lysine) at 32°C. All strains were constructed using transformations and/or crosses. For the genetic selection, the two reporter genes were constructed individually and then crossed to each other. The *FLO8-URA3* reporter was constructed by inserting the *URA3* gene at the 3′ end of the *FLO8* gene, replacing base pairs +1727 – +2505 (+1 = ATG) (22). The *STE11-CAN1* reporter was constructed by inserting the *CAN1* gene at the 3′ end of the *STE11* gene, replacing base pairs +1871 - +2154 (+1 = ATG) (50). In the same strain, the coding sequence of the endogenous *CAN1* gene was deleted using

a HygMX cassette, which was amplified from the *pFA6a-hphMX6* plasmid (51). To make the strain containing the *STE11-CAN1* reporter amenable to crosses, the *STE11-TAP-HIS3MX* cassette was amplified from a strain derived from the yeast TAP-tagged collection (52) and inserted at the *HO* locus replacing base pairs −1400 to +1761 (+1 = ATG). For spot tests to check for reporter expression, cells were spotted on media containing 1 mg/ml 5-FOA and/or 150 µg/ml canavanine unless mentioned otherwise. For verification of mutants obtained from the selection, point mutations were made in the *SET2* gene by two-step gene replacement (53) in a strain containing only the *STE11-CAN1* reporter. The same strategy was used to make the different deletions within the region of the *SET2* gene that encodes the autoinhibitory domain. For Spt6 depletion experiments, cells were grown to $OD_{600} \approx 0.6$ (~2×10^7 cells). Cells were diluted in YPD to $OD_{600} = 0.3$. A fraction of the diluted culture was collected and treated as the 0 min time point. Indole acetic acid dissolved in ethanol was then added to the medium at a final concentration of 25 µM and cultures were grown at 30°C. Cells were collected at 90, 120 and 150 min to prepare whole cell extracts for western blotting.

Isolation and analysis of mutants that suppress intragenic transcription

The genetic selection for isolating mutants that suppress intragenic transcription in *spt6-1004* was done in two rounds. In the first round, 25 independent cultures each of FY3129 and FY3130 were grown to saturation overnight in YPD. Cells were washed twice with water and $2–4 \times 10^7$ cells from each independent culture were spread on two SC-Arg plates containing 0.25 mg/ml 5-FOA and 150 µg/ml canavanine, one of which was UV irradiated. All plates were incubated at 34°C, which reduced background growth, and colonies that grew between days 3 and 7 were picked for further analysis. The second round of selection was identical to the first round, except that cells were plated on SC-Arg plates containing 0.5 mg/ml 5-FOA and 150 µg/ml canavanine. To test for dominance, the suppressor strains were first crossed with the parent *spt6-1004* strain carrying both the reporters, diploids were selected by complementation, and the purified diploids were tested for growth on a medium containing 5-FOA and canavanine. To test for linkage, suppressors were crossed to each other, sporulated, and tetrads were dissected and analyzed by standard conditions. At least 10 tetrads were analyzed per cross.

Identification of suppressor mutations by whole-genome sequencing

Eight of the twenty independent dominant mutants identified were subjected to further genetic analysis and found to contain mutations in a single gene responsible for the suppression phenotype. Whole genome sequencing libraries were prepared for the eight mutants and two parents (FY3129 and FY3130) as described previously (54). Sonication of genomic DNA was done using Covaris S2 (3 cycles of 50''; Duty cycle: 10%; Intensity: 4; Cycles/burst: 200) to obtain fragments between 100 and 500 bp. GeneRead DNA library prep kit (QIAGEN) was used for end repair,

A tailing and adapter ligation. The DNA samples were purified twice using 0.7x volume SPRI beads. PCR cycles for final amplification were selected based on trial amplification runs. Following the final PCR, DNA was purified twice using $0.7\times$ volume SPRI beads and submitted for next-generation sequencing. Sequencing was done on an Illumina Hi-Seq platform. Reads from the FASTQ file were aligned using Bowtie2 (55) (default parameters) and variants between all 10 libraries and the reference genome were called using the *samtools mpileup* command (56). The resulting VCF file was then used to identify variants that were present only in the mutants and not in the parents using a custom R script (https://github.com/winston-lab/wgs_snp_analysis_2018). All variants that mapped within the coding sequence of a gene were identified. The gene that had variants in all mutants was found to be *SET2*.

Spot tests

Yeast cultures were grown overnight from single colonies. Cells were pelleted and washed once with water. All cultures were normalized by their OD_{600} values and six 10-fold serial dilutions of each culture were made in a 96-well plate. The cultures were spotted on different media and incubated at the appropriate temperatures. All plates containing FOA and/or canavanine were incubated at $34°C$ to ensure higher stringency for assaying intragenic transcription. The control complete plates for these experiments were also incubated at $34°C$. The Spt⁻ phenotype was assayed at $30°C$. Temperature sensitivity was assayed at $37°C$. For mutant backgrounds with weak intragenic transcription (as in Figure 5), expression of the *FLO8-URA3* reporter was tested on SC-Ura medium.

Western blotting and antibodies

Saccharomyces cerevisiae cells were grown to $OD_{600} \approx 0.6$ ($\sim 2 \times 10^7$ cells). Culture volumes were normalized by their OD_{600} such that an OD equivalent (OD_{600} * volume of the culture) of 6 was harvested. The cell pellets were washed once with water and suspended in 300 µl water. Then, 300 µl of 0.6 M sodium hydroxide was added to the cells, and the suspension was incubated at room temperature for 10 min. The cells were then pelleted and resuspended in 80 µl Modified SDS buffer (60 mM Tris–HCl, pH 6.8, 4% β-mercaptoethanol, 4% SDS, 0.01% bromophenol blue and 20% glycerol) (57). Eight microliters of the extracts were loaded on sodium dodecyl sulphate-polyacrylamide gel electrophoresis (SDS-PAGE) gels for western blotting. *Schizosaccharomyces pombe* cells were grown to $OD_{600} \approx$ 0.6 ($\sim 10^7$ cells/ml). Ten milliliters of cells were pelleted and resuspended in 200 µl of 20% trichloroacteric acid (TCA). Next, 200 µl of glass beads were added to the tube and the cells were lysed by bead beating for 2 min at 4°C. The bottom of the tube was punctured and the flow through collected by centrifugation. The beads were washed twice with 200 µl of 5% TCA and the flow through was collected. The pooled flow through fractions were spun at 3000 rpm for 10 min at room temperature and the resulting pellet was resuspended in 150 µl (normalized by OD_{600}; culture of OD_{600} = 0.8 was suspended in 150 µl) of 2x Laemmli buffer (125

mM Tris–HCl, pH 6.8, 4% SDS, 10% β-mercaptoethanol, 0.01% bromophenol blue, 40% glycerol). An equal volume of 1 M Tris base (pH not adjusted) was added to neutralize the TCA. The samples were incubated for 5 min at 95°C and spun down at 10 000 rpm for 30 s. Then, 10 µl of the supernatant was loaded on an SDS-PAGE gel for western blotting. Primary antibodies used for western blotting were: anti-Set2 (1:8000, generously provided by Brian Strahl), anti-H3K36me3 (1:2000, Abcam, ab9050), anti-H3K36me2 (1:2500, Abcam, ab9049) or (1:1000, Upstate #07-274), anti-HA (1:5000, Abcam, ab9110), anti-Flag (1:5000, Sigma, F3165), anti-H3 (1:2500, Abcam, ab1791), anti-V5 (1:5000, Invitrogen, R960-25), anti-Pgk1 (1:10 000, Life Technologies 459250) and anti-Act1 (1:10 000, Abcam, ab8224). Secondary antibodies used were: goat anti-rabbit IgG (1:10 000, Licor IRDye 680RD) and goat anti-mouse IgG (1:20 000, Licor, 800CW). Quantification of western blots was done using Licor ImageStudio software.

Northern blotting

RNA extraction from *S. cerevisiae* was done using hot acid phenol extraction as described previously (58). Northern blotting was done as described previously (58) with many modifications. Fifteen micrograms of RNA was loaded per sample. The composition of the final RNA loading dye was 6% formaldehyde, $1\times$ MOPS, 2.5% Ficoll, 10 mM Tris–HCl, pH 7.5, 10 mM EDTA, 7 µg/ml ethidium bromide, 0.025% bromophenol blue and 0.025% Orange G. Following the addition of RNA loading dye, the RNA sample was heated at 65°C for 5 min and then transferred to ice before loading on the gel. Transfer of the RNA from gel to the membrane was done using upward capillary transfer in $1\times$ SSC solution. Pre-hybridization of the membrane was done for 3 to 5 h in pre-hybridization solution (50% deionized formamide, 10% dextran sulphate, 1 M NaCl, 0.0 5M Tris–HCl, pH 7.5, 0.1% SDS, 0.1% sodium pyrophosphate, $10\times$ Denhardts reagent, 500 µg/ml denatured salmon sperm DNA) at 42°C. Following hybridization, six washes were done: 2 washes with $2\times$ SSC solution at room temperature for 15 min each, 2 washes with $2\times$ SSC, 0.5% SDS at 65°C for 30 min each and 2 washes with $0.1\times$ SSC at room temperature for 30 min each. Probes were made with the PCR primers listed in Supplementary Table S2.

Cloning and expression of Set2 protein in insect cells

All plasmids used in this study are listed in Supplementary Table S3. For creating the GST-Set2 bacmids, full-length wild-type *SET2* or *SET2-H366N* was PCR amplified and first cloned into the BamHI/XhoI sites of the pGEX6p1 vector producing FB2798 and FB2799. This resulted in fusing the GST tag to the N-terminal end of Set2, with the presence of a Prescission protease site between the tag and the protein. The *GST-SET2* constructs were cloned into the pFastBac1 vector by Gibson cloning (59) using a 40-bp overlapping sequence between the amplified vector and insert producing FB2800 and FB2801. These plasmids were then transformed into DH10Bac *Escherichia coli* cells, and transformants that had inserted the GST-Set2 constructs into the bacmid were identified by blue-white screening,

producing FB2802 and FB2803 that were then used for transfecting Sf9 cells. Sf9 transfection with bacmid DNA and virus amplification were performed essentially as described for the Bac-to-Bac Baculovirus Expression System (ThermoFisher Scientific). Sf9 cells were maintained in ESF 921 insect cell culture medium (Expression Systems, 96-001-01) supplemented with 50 U/ml Penicillin–Streptomycin (ThermoFisher Scientific, 15140-122). For protein expression, 2×10^6 Sf9 cells/ml were infected at a multiplicity of infection of ~10. Cells were harvested 66 h post-infection by centrifugation at $5000 \times g$ for 15 min.

Purification of Set2 from insect cells

The cell pellet from 100 ml of Sf9 cells was lysed with 20 ml of BV lysis buffer (50 mM HEPES, pH 7.9, 500 mM NaCl, 10% glycerol, 0.5 mM EDTA, 2 mM MgCl$_2$ and 0.2% Triton X-100) on ice for 30 min. The cell lysate was then spun at 40 000 rpm for 30 min at 4°C. The supernatant was added to 100 μl of glutathione sepharose beads (GE, 17075601) pre-washed twice in BV lysis buffer and incubated at 4°C with gentle shaking for 2 h. The beads were washed twice with 20 ml of BV lysis buffer, and twice with 20 ml of Prescission buffer (50 mM Tris–HCl, pH 8.0, 150 mM NaCl, 1 mM EDTA, 10% glycerol) that contained 0.005% Triton X-100 to help pellet the beads. The beads were then suspended in 1 ml of Prescission buffer. Four microliters of Prescission protease (GE, 27084301) were added to the beads that were then incubated at 4°C overnight with end-over-end rotation. The beads were then spun down and the supernatant, which had the eluted protein, was concentrated in Amicon columns to a volume of ~80 μl. Protein concentrations were estimated by Bradford assay (60), and equivalent amounts of protein were analyzed on an SDS-PAGE gel along with a bovine serum albumin standard to confirm this measurement. The proteins were frozen in aliquots at −70°C.

Histone methyltransferase assays

Histone methyltransferase assays were done based on a previously described method (49). Assays were carried out in 10 μl reactions. Purified Set2 protein (at a final concentration of 0.23, 0.46 or 0.94 μM) was mixed with 1 μl ^{3}H S-adenosyl methionine (55-85 Ci/mMole, Perkin Elmer, NET155H250UC) and 1 μg of recombinant Xenopus nucleosomes in a buffer that had a final composition of 50 mM Tris, pH 8.0, 75 mM NaCl, 1 mM MgCl$_2$, 2 mM DTT and 5% glycerol. The reactions were incubated at 30°C for 1 h. The reactions were then spotted on half of a P81 phosphocellulose filter paper circle (Whatman) and allowed to dry. The filters were washed three times in 50 ml HMT Wash buffer (39 mM NaHCO$_3$, 11 mM Na$_2$CO$_3$, pH 9.2). The filters were briefly rinsed in acetone and allowed to air dry. The filters were then placed in scintillation vials containing 4 ml scintillation fluid (RPI, 111167) and scintillation counting was done in a Beckman Coulter LS 6500 machine for 1 min.

ChIP and ChIP-Seq

For *S. cerevisiae* cultures, 140 ml of cells were grown to OD$_{600}$ ≈ 0.6 (~2×10^7 cells) in YPD. Cultures were cross-

linked by the addition of formaldehyde to a final concentration of 1% followed by incubation with shaking at room temperature for 20 min. Glycine was added to a final concentration of 125 mM and the incubation was continued for 10 min. The cells were pelleted and washed twice with cold $1\times$ TBS (100 mM Tris, 150 mM NaCl, pH 7.5) and once with cold water. The cell pellets were then suspended in 800 μl cold LB140 buffer (50 mM HEPES-KOH, pH 7.5, 140 mM NaCl, 1 mM EDTA, 1% Triton X-100, 0.1% sodium deoxycholate, 0.1% SDS, $1\times$ cOMPLETE Protease Inhibitor tablet (Roche)). One milliliter of glass beads were added and the cells were lysed by bead beating for 8 min at 4°C with incubation on ice for 3 min after every 1 min. The lysate was collected and centrifuged at 12 500 rpm for 5 min and the resulting pellet was washed once with 800 μl cold LB140 buffer. The pellet was resuspended in 580 μl cold LB140 buffer and sonicated in a QSonica Q800R machine for 20 min (30 s on, 30 s off, 70% amplitude). The sonicated samples were centrifuged at 12 500 rpm for 30 min and the resulting supernatant was taken for the immunoprecipitation step. For the *S. pombe* spike-in strain, 120 ml of cells were grown to OD$_{600}$ ≈ 0.6 in YES and processed similar to the *S. cerevisiae* culture except for the following steps: bead beating for cell lysis was done for 11 min. Sonication was done for 15 min. The protein concentrations in chromatin were measured by Bradford assay (60). About 300–500 μg of *S. cerevisiae* chromatin was mixed with 33–55 μg (10%) of *S. pombe* chromatin, and the volume was brought up to 800 μl with WB140 buffer (50 mM HEPES-KOH, pH 7.5, 140 mM NaCl, 1 mM EDTA, 1% Triton X-100, 0.1% sodium deoxycholate). This was used as the input for the immunoprecipitation reaction. Antibody (amounts mentioned below) was added to the input and the samples incubated overnight at 4°C with end-over-end rotation. About 50 μl of Protein G sepharose beads (GE Healthcare) pre-washed twice in WB140 were added to the IPs and samples were incubated for 4 h at 4°C with end-over-end rotation. The beads were washed twice with WB140, twice with WB500 (50 mM HEPES-KOH, pH 7.5, 500 mM NaCl, 1 mM EDTA, 1% Triton X-100, 0.1% sodium deoxycholate), twice with WBLiCl (10 mM Tris, pH 7.5, 250 mM LiCl, 1 mM EDTA, 0.5% NP-40, 0.5% sodium deoxycholate) for 2 min each and once with TE (10 mM Tris, pH 7.4, 1 mM EDTA) for 5 min. The immunoprecipitated material was eluted twice with 100 μl TES (50 mM Tris, pH 7.4, 10 mM EDTA, 1% SDS) at 65°C for 30 min. The eluates were incubated at 65°C overnight to reverse the crosslinking. Two hundred microliters of TE was added to the eluates followed by RNase A/T1 to a final concentration of 0.02 μg/μl. The samples were incubated at 37°C for 2 h. Proteinase K was added to a final concentration of 0.4 mg/ml and samples were incubated at 42°C for 2 h. DNA was purified using Zymo DCC (for ChIP-Seq) or EZNA Cycle Pure kit spin columns (for ChIP-qPCR). The purified DNA was used for qPCR or library preparation for next-generation sequencing. Primers used for qPCR are listed in Supplementary Table S2. The library preparation steps from this stage were similar to those used for preparation of DNA libraries for whole genome sequencing (54). Next-generation sequencing was done on an Illumina NextSeq platform. About 5 μl of anti-HA (Abcam, ab9110) per 500 μg of chromatin, 10

μl (5 μl for ChIP-qPCR) of anti-Rpb1 (Millipore, 8WG16) per 500 μg of chromatin, 4 μl of anti-H3 (Abcam, ab1791) per 300 μg of chromatin, 4 μl of anti-H3K36me2 (Abcam, ab9049) per 300 μg of chromatin, 4 μl of anti-H3K36me3 (Abcam, ab9050) per 300 μg of chromatin and 50 μl of anti-FLAG M2 affinity gel (Sigma, #A2220) per 500 μg of chromatin were used for ChIP. HA tagged Set2 was used for all ChIP-seq and follow-up ChIP-qPCR experiments. FLAG tagged Set2 was used for ChIP-qPCR of *set2* mutants lacking the SRI and HB domains.

ChIP-seq computational analysis

A custom ChIP-seq pipeline was generated using the Snakemake workflow manager (61). ChIP-seq data were aligned to a combined *S. cerevisiae* + *S. pombe* genome using Bowtie2 (55). About 72–93% of the reads mapped exactly once to the combined genome. The number of mapped reads for *S. cerevisiae* IPs (excluding inputs) varied from 1 to 10 million reads. The number of mapped reads for *S. pombe* immunoprecipitation (excluding inputs) varied from 0.35 to 6 million reads. Cross correlation was done using SPP package (62) to estimate fragment sizes for the different libraries. The coverage files were produced using the igvtools count function (63), extending reads by (length of fragment sizes − average read length) for each library. Spike in normalization was done as described previously (64), correcting for variations in the input samples. Correlation plots, heat maps and metagene plots were produced using custom R scripts. To identify genes that did not show rescue of H3K36me2 in the suppressor strain, coverage within 20 bp windows tiling the entire genome was generated for each library. IP libraries were divided by their respective control libraries after the addition of a pseudocount of one. The mean coverage over every gene in each library was determined using the bedtools map command (65). The ratio of the mean coverage for every gene in one sample over the other was calculated. All code used to analyze the data can be found at https://github.com/winston-lab/chip-seq-analysis-pipeline.

RESULTS

Isolation and analysis of dominant *SET2* mutations that suppress intragenic transcription in an *spt6-1004* mutant

To identify factors that regulate intragenic transcription, we selected for mutations that suppress this class of transcription in an *spt6-1004* mutant (21), which allows extensive intragenic transcription (22,23,25). To select for suppressors, we constructed two reporters using characterized intragenic transcription start sites in the *FLO8* (21) and *STE11* (50) genes (Figure 1A and B; 'Materials and methods' section). In the *FLO8-URA3* reporter, intragenic transcription confers sensitivity to 5-FOA, while in the *STE11-CAN1* reporter, intragenic transcription confers sensitivity to canavanine. To select for mutations that suppress intragenic transcription, we constructed *spt6-1004* strains that contained both reporters and selected for resistance to both 5-FOA and canavanine (5-FOA^R Can^R). The double selection reduced the likelihood of isolating *cis*-acting mutations

in either reporter, thereby enriching for mutants that generally affect intragenic transcription.

We isolated and characterized 20 independent mutants. By standard genetic tests, we showed that all 20 mutations were dominant. We then tested eight mutants by crosses and showed that the 5-FOA^R Can^R phenotype was caused by a single mutation in each strain and that the mutations were tightly linked to each other, with no recombinants found in any of seven crosses (10 tetrads/cross). To identify candidate mutations, we performed whole genome sequencing of these eight suppressor strains and identified single base pair changes in the *SET2* gene in all eight mutants, suggesting that these are the causative mutations that suppress intragenic transcription. Sequencing of the *SET2* gene in the other 12 suppressors also revealed mutations in *SET2*. The 20 mutations (Figure 1C, Supplementary Table S4) are clustered within a small region of *SET2* encoding a previously identified autoinhibitory domain (49).

To verify that the dominant *SET2* mutations are causative for suppression of intragenic transcription in *spt6-1004*, we recreated three of the identified *SET2^{sup}* mutations in the *spt6-1004* parental reporter strains. As 13 of the 20 *SET2^{sup}* mutations are within three adjacent codons (365–367) (Figure 1C), we decided to test three of these mutations, *SET2-L365Q*, *SET2-H366N* and *SET2-G367S*, and a fourth mutation (*SET2Δ3*) that deleted these three *SET2* codons. In all four cases, the reconstructed mutants were 5-FOA^R and Can^R, showing that each of the *SET2* mutations was causative (Figure 1D). Suppression was specific for intragenic transcription as the mutants still had other *spt6* mutant phenotypes, including Spt$^-$ and temperature-sensitive growth (Figure 1D). To assay the effect of a *SET2^{sup}* mutation on levels of an intragenic transcript, we performed northern blots, looking at *STE11* transcripts, using a strain with a wild-type *STE11* gene. Our results showed that the *SET2Δ3* mutation strongly suppressed *STE11* intragenic transcript levels in an *spt6-1004* mutant, to levels similar to that in wild-type cells (Figure 1E). Deletion of the entire *SET2* gene does not suppress intragenic transcription in an *spt6-1004* background (Figure 1E), demonstrating that our *SET2^{sup}* mutations do not cause loss of Set2 activity. Suppression by the *SET2Δ3* mutation suggests that the suppression phenotype occurs by impairment of the Set2 autoinhibitory domain. Taken together, our results show that mutations that change or remove amino acids in the Set2 autoinhibitory domain suppress intragenic transcription in an *spt6-1004* mutant.

SET2^{sup} mutations rescue H3K36 di- and trimethylation in an *spt6-1004* mutant

Given that all of our suppressor mutations were in *SET2*, we tested whether they suppress the H3K36me2/me3 defect in *spt6-1004*, using quantitative western blots. Compared to the *spt6-1004* single mutant, where H3K36me3 is undetectable, our results show that four different *SET2^{sup} spt6-1004* double mutants have a substantial level of H3K36me3, ∼10–40% of the level of a wild-type strain (Figure 2A and B). In addition, all of the other originally isolated *SET2^{sup}* mutants, tested once, restored H3K36me3 to varying extents in an *spt6-1004* background (data not shown). Fur-
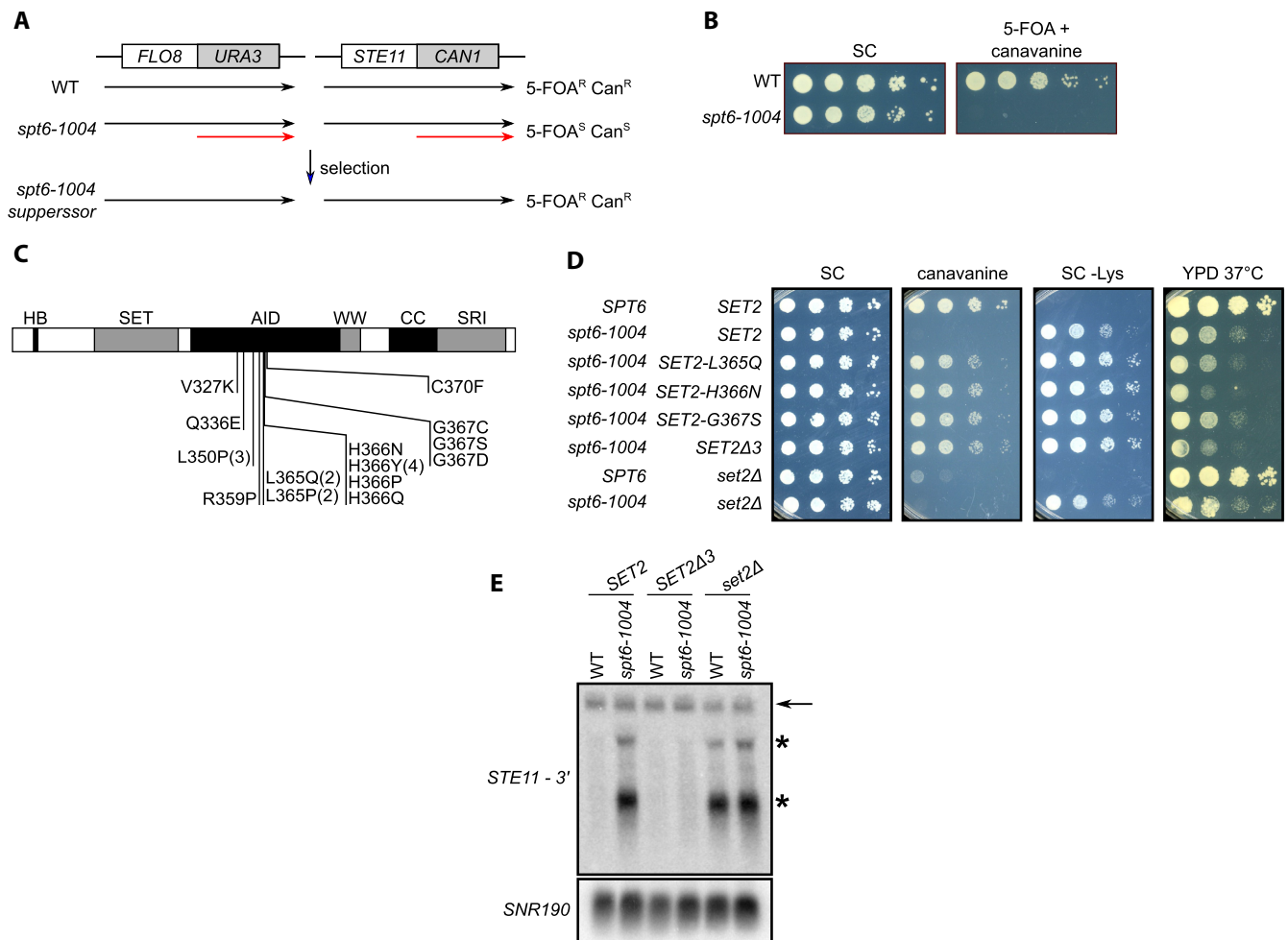
Figure 1. Isolation of mutations that suppress intragenic transcription in *spt6-1004*. (**A**) Shown at the top are diagrams of the two reporters and the selection used to isolate suppressor mutations. Shown below each are the transcripts made in wild-type (WT), *spt6-1004* and *spt6-1004* strains with a suppressor. In *spt6-1004* mutants, the *FLO8-URA3* reporter confers 5-FOA sensitivity and the *STE11-CAN1* reporter confers canavanine sensitivity due to expression of the intragenic transcripts, shown in red. (**B**) Spot tests of cells grown at 34°C that show the selective conditions for the mutant selection. (**C**) A diagram of the Set2 protein that depicts the amino acid changes caused by the dominant *SET2sup* mutations. The numbers in parentheses indicate the number of times the same mutation was isolated if more than once. One isolate had two point mutations that coded for L365P and H366Y in the same protein. The letters above the rectangle indicate the identified domains in Set2: HB, histone binding domain; SET, the catalytic domain; AID, the autoinhibitory domain; the WW domain; CC, a coiled coil motif; SRI, the Set2 Rpb1 interacting domain. (**D**) Spot tests of cells grown at 34°C to assay suppression of intragenic transcription in *spt6-1004* by SET2sup mutations using the *STE11-CAN1* reporter. (**E**) Northern analysis of the *STE11* gene, using a probe from the 3′ region of *STE11*, to assay the suppression of intragenic transcription in *spt6-1004* by a *SET2sup* mutation. In wild-type, there is a single full-length *STE11* transcript (denoted by the arrow), while in the *spt6-1004* mutant, there are two intragenic transcripts (denoted by the asterisks) in addition to the full-length transcript. *SNR190* served as the loading control.

thermore, we constructed a series of short deletions that removed segments of the Set2 autoinhibitory domain and found that they also suppressed the H3K36me2/me3 defect in *spt6-1004* to a similar degree as the *SET2sup* mutations (Supplementary Figure S1). Thus, multiple types of changes in the Set2 autoinhibitory domain partially bypass the requirement of Set2 for Spt6.

To determine the effect of a *SET2sup* mutation in an otherwise wild-type background, we compared the effects of the *SET2Δ3* mutation on H3K36me2 and H3K36me3 levels with and without an *spt6-1004* mutation. In an *spt6-1004 SET2Δ3* double mutant, H3K36me3 levels are ~25% of wild-type levels and H3K36me2 levels are ~150% of wild-type (Figure 2C and D). In the *SET2Δ3* single mutant, there

appears to be hyperactivation of Set2 activity, as we observed greater levels of H3K36me3 and slightly decreased levels of H3K36me2 compared to wild-type (Figure 2C and D). Importantly, these changes in H3K36 methylation are not caused by elevated levels of Set2 protein (Figure 2E). Taken together, our results suggest that the Set2 autoinhibitory domain makes Set2 activity dependent upon Spt6.

To test whether *SET2sup* mutations can also suppress depletion of the Spt6 protein in addition to suppressing the *spt6-1004* mutation, we conditionally depleted Spt6 via an auxin-inducible degron (66). In a wild-type *SET2* background, as expected, we observed decreased levels of H3K36me2/me3 upon Spt6 depletion (Supplementary Figure S2). Set2 levels also decreased during the time course
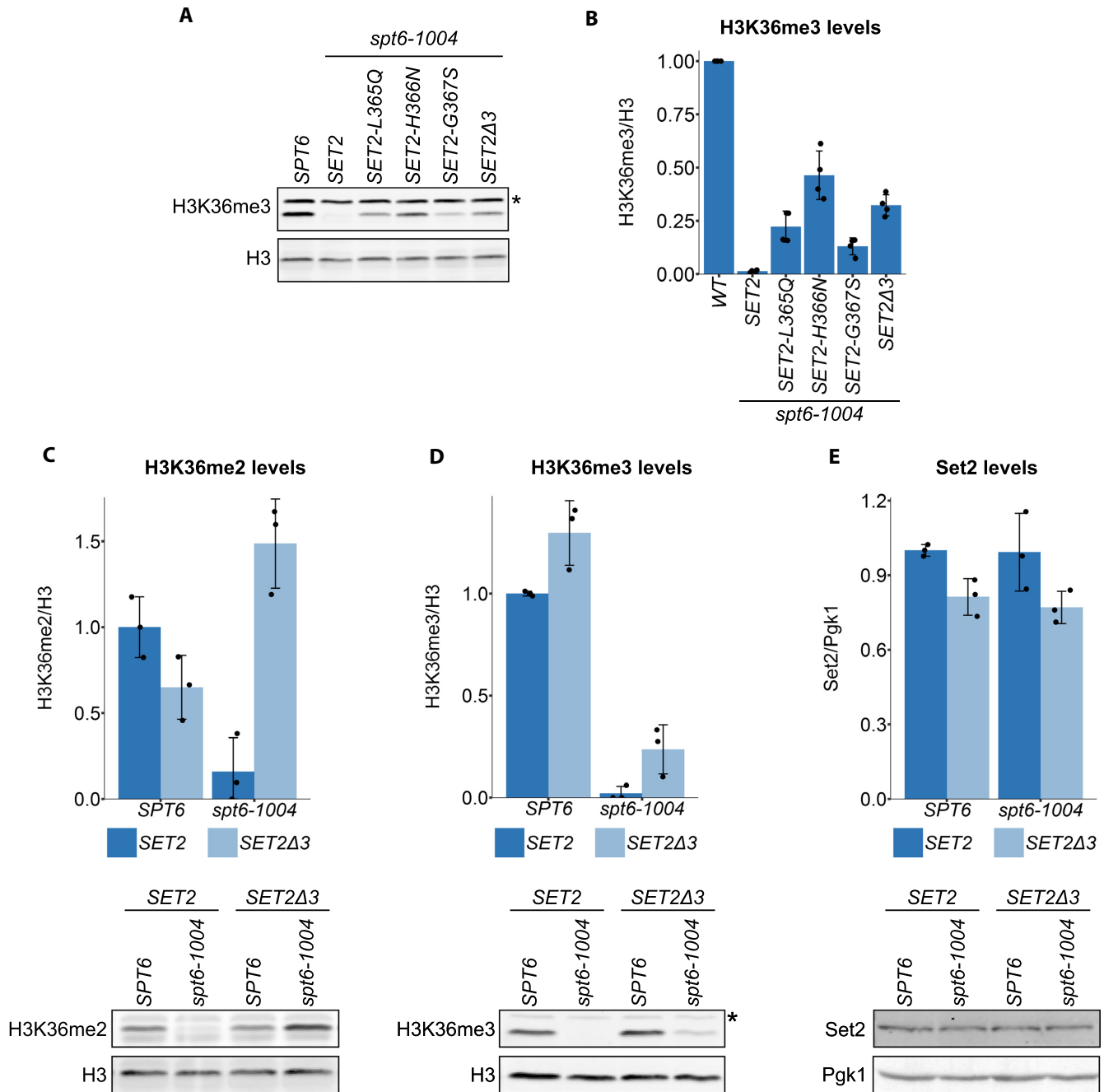
Figure 2. *SET2^sup* mutations suppress the H3K36 methylation defect in *spt6-1004*. (**A**) A western blot showing the levels of H3K36me3 and total histone H3 in four different *SET2^sup* mutants. The asterisk denotes a non-specific band. (**B**) Quantification of H3K36me3 relative levels of the strains shown in (A). (**C-E**) Quantification of western blots assaying the levels of H3K36me2 (C), H3K36me3 (D) and Set2 (E) in wild-type and *spt6-1004* strains with or without the *SET2Δ3* mutation, normalized to their respective loading controls. For all bar graphs, the black dots represent the individual data points for three experiments and the bars show the mean ± standard deviation. A representative western blot is shown below each bar graph.

of this experiment, although this occurs later than the loss of H3K36 methylation. When Spt6 is depleted in the *SET2Δ3* background, we observed increased levels of H3K36me2/me3 during the depletion compared to the wild-type *SET2* background, although the levels eventually decreased as Set2 protein levels decreased. Despite the decreasing levels of Set2, these results show that *SET2^sup* mu-

tations partially bypass the H3K36me2/me3 defects caused by depletion of Spt6.

SET2^sup mutations suppress *spt6-1004* via the Set2/Rpd3S pathway

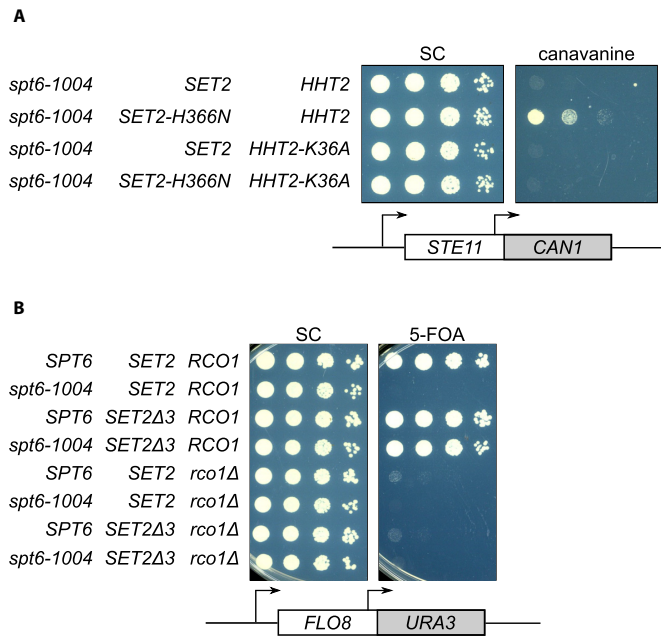We also performed two sets of experiments to verify that the *SET2^sup* mutations function via H3K36 methylation and

Figure 3. *SET2^sup* mutations suppress *spt6-1004* via the Set2/Rpd3S pathway. (**A**) Spot tests of cells grown at 34°C assaying expression of the *STE11-CAN1* reporter, showing the effect of the H3K36A mutation on the suppression phenotype. (**B**) Spot tests of cells grown at 34°C, assaying the effect of *rco1Δ* on the expression of the *FLO8-URA3* reporter in suppressor strains.

Figure 4. *SET2-H366N* is hyperactive *in vitro*. (**A**) Coomassie-stained gel loaded with equivalent amounts of purified wild-type Set2 and Set2-H366N. (**B**) Histone methyltransferase assays showing ³H incorporation in the presence of wild-type Set2 and Set2-H366N. The dots represent individual data point for three experiments and bars show mean ± standard deviation. A similar result was obtained using independent preparations of wild-type and mutant Set2 proteins.

the function of Rpd3S. First, to confirm that the *SET2^sup* mutations exert their phenotype by restoring methylation of H3K36 rather than by some other event, we compared *spt6-1004 SET2-H366N* strains that express either wild-type histone H3 or an H3K36A mutant. Our results showed that the *spt6-1004 SET2-H366N* strain expressing H3K36A was no longer able to suppress intragenic transcription (Figure 3A); therefore, H3K36 methylation is necessary for the suppression of intragenic transcription. Second, as H3K36me2/me3 is required for the function of the Rpd3S histone deacetylase complex (17,37–40), we assayed whether suppression of *spt6-1004* required a functional Rpd3S complex, by testing a strain lacking the Rpd3S component Rco1. Our results showed that *rco1Δ* reversed the suppression phenotype, similar to the H3K36A mutant (Figure 3B), showing that functional Rpd3S is necessary for the suppression of intragenic transcription by *SET2^sup* mutations. Together, these results demonstrate that methylation at H3K36 and the subsequent activation of Rpd3S confer suppression by the *SET2^sup* mutations.

SET2^sup mutations show greater activity *in vitro*

Given our observation of higher H3K36me3 levels in *SET2Δ3* cells as compared to wild-type, we hypothesized that *SET2^sup* mutations compromise the function of the autoinhibitory domain and thereby make Set2 hyperactive. To directly test this hypothesis, we expressed and purified wild-type Set2 and Set2-H366N from insect cells. The purification strategy involved the use of a cleavable GST tag that permitted us to purify full-length Set2 with the presence of only five additional amino acids at the N-terminal end (Fig-
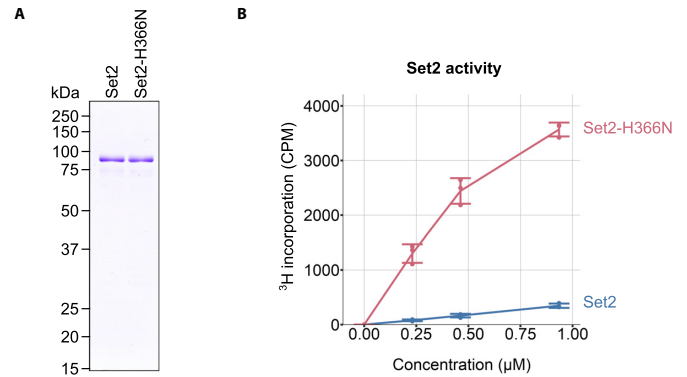
ure 4A). *In vitro* histone methyltransferase assays using purified Set2 and recombinant Xenopus mono-nucleosomes showed much greater activity for Set2-H366N compared to wild-type Set2 (Figure 4B). Both proteins showed increased methyltransferase activity with higher concentration of enzyme, and the differential activity between the wild-type and mutant enzymes was maintained throughout the range of concentrations. This result suggests that rescue of H3K36 methylation by *SET2^sup* mutations in *spt6-1004* cells is due to greater activity of Set2 and not due to altered expression or activity of a different factor in the mutant.

SET2^sup mutations suppress H3K36 methylation defects that occur in other transcription elongation factor mutants

We wanted to test whether *SET2^sup* mutations can suppress the loss of other functions that are required for both H3K36 methylation and repression of intragenic transcription. In particular, we tested the PAF complex and Ctk1 which, along with Spt6, have been proposed to be part of a feed-forward mechanism that regulates transcription elongation (67). For the PAF complex, we tested *paf1Δ* and *ctr9Δ*, both of which cause loss of H3K36me3, with no detectable effect on either H3K36me2 or Set2 protein levels (Figure 5A–C) (42). *SET2Δ3* strongly suppressed the H3K36me3 defect of both *paf1Δ* and *ctr9Δ* (Figure 5B). In a *ctk1Δ* mutant, there are decreased Set2 protein levels and loss of both H3K36me3 and H3K36me2 (Figure 5A–C) (19,43,67). *SET2Δ3* strongly suppressed the H3K36me2 defect in *ctk1Δ*, restoring it to a level greater than in wild-type strains (Figure 5A), although it had no effect on H3K36me3 or on the diminished Set2 protein levels (Figure 5B and C). We also tested whether *SET2Δ3* suppresses intragenic transcription in these mutants. Our results showed that *SET2Δ3* suppressed intragenic transcription in *paf1Δ* and *ctr9Δ* mutants, but not in the *ctk1Δ* mutant (Figure 5D). The latter result suggests that restoration of H3K36me2 but not H3K36me3 in *ctk1Δ* is insufficient for the repression of intragenic transcription. The bypass of the requirements for multiple factors by *SET2^sup* mutations suggests that the
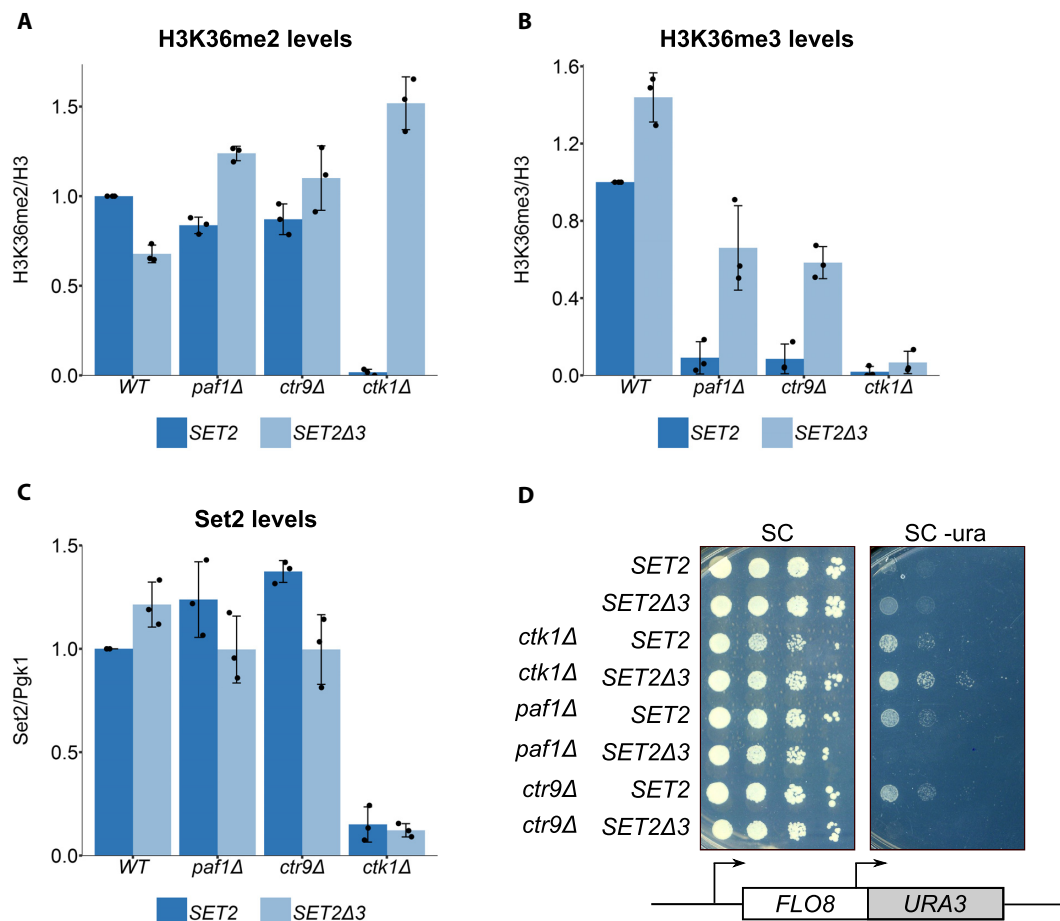
Figure 5. *SET2Δ3* suppresses the H3K36me2/me3 defects in *ctk1Δ, paf1Δ and ctr9Δ*. (**A–C**) Quantification of western blots assaying H3K36me2 (A), H3K36me3 (B) and Set2 (C) levels in the indicated mutants with or without the *SET2Δ3* mutation, normalized to their respective loading controls. The black dots represent the individual data points for three experiments, and the bars show the mean ± standard deviation. (**D**) Spot tests of cells grown at 30°C, assaying the effect of the *SET2Δ3* mutation on the expression of *FLO8-URA3* reporter in the indicated mutants. Since intragenic transcription is weak in these mutants, growth has been assayed on SC-Ura medium (see 'Materials and methods' section).

Set2 autoinhibitory domain confers dependence upon these factors for Set2 function.

SET2^{sup} mutations suppress the loss of Set2 domains normally required for its catalytic activity

We also investigated whether *SET2*^{sup} mutations suppress the loss of two Set2 regulatory domains required for Set2 activity: the SRI domain, which binds to the RNAPII CTD (19,48), and the HB domain, required for interaction with histones H2A and H4 (45). To do this, we deleted portions of the *SET2* gene to remove one or both domains in the Set2 protein in a wild-type *SET2* gene and a *SET2Δ3* mutant (Figure 6A). We then tested the new mutants for levels of H3K36me2, H3K36me3 and Set2. Our results showed that *SET2Δ3* suppresses both the *set2ΔSRI* and *set2ΔHB* mutations with respect to their H3K36 methylation defects (Figure 6A and Supplementary Figure S3). However, *SET2Δ3* is unable to rescue H3K36 methylation in a *set2ΔHB,ΔSRI* double mutant. This is not due to either altered recruitment or the level of the mutant protein (Figure 6B and Supplementary Figure S3C). Consistent with the H3K36 methylation levels, *SET2Δ3* was able to sup-

press intragenic transcription in a *set2ΔSRI* but not in a *set2ΔHB,ΔSRI* strain (Figure 6C). Our results suggest that the Set2 autoinhibitory domain monitors the interactions of the Set2 SRI and HB domains with RNAPII and nucleosomes, respectively.

The regulation of Set2 activity by Spt6 and Set2^{sup} mutants occurs at a step after the recruitment of Set2 to chromatin

Although the H3K36 methylation defect in *spt6-1004* mutants was discovered several years ago, there is little understanding of why Spt6 is required for this histone modification. Our *spt6-1004* strains, when grown at 30°C, have almost normal Set2 levels (Figure 2E and Supplementary Figure S4C); however, H3K36me2 and H3K36me3 are undetectable. Therefore, the requirement for Spt6 must be at a step other than regulation of Set2 stability. Two other possible mechanisms for regulation include the recruitment of Set2 to chromatin or the regulation of Set2 activity after its recruitment. To distinguish between these possibilities, as well as to better understand the suppression of *spt6-1004* by *SET2*^{sup} mutations, we performed ChIP-seq for Set2-HA, Rpb1, H3K36me3, H3K36me2 and total H3. These
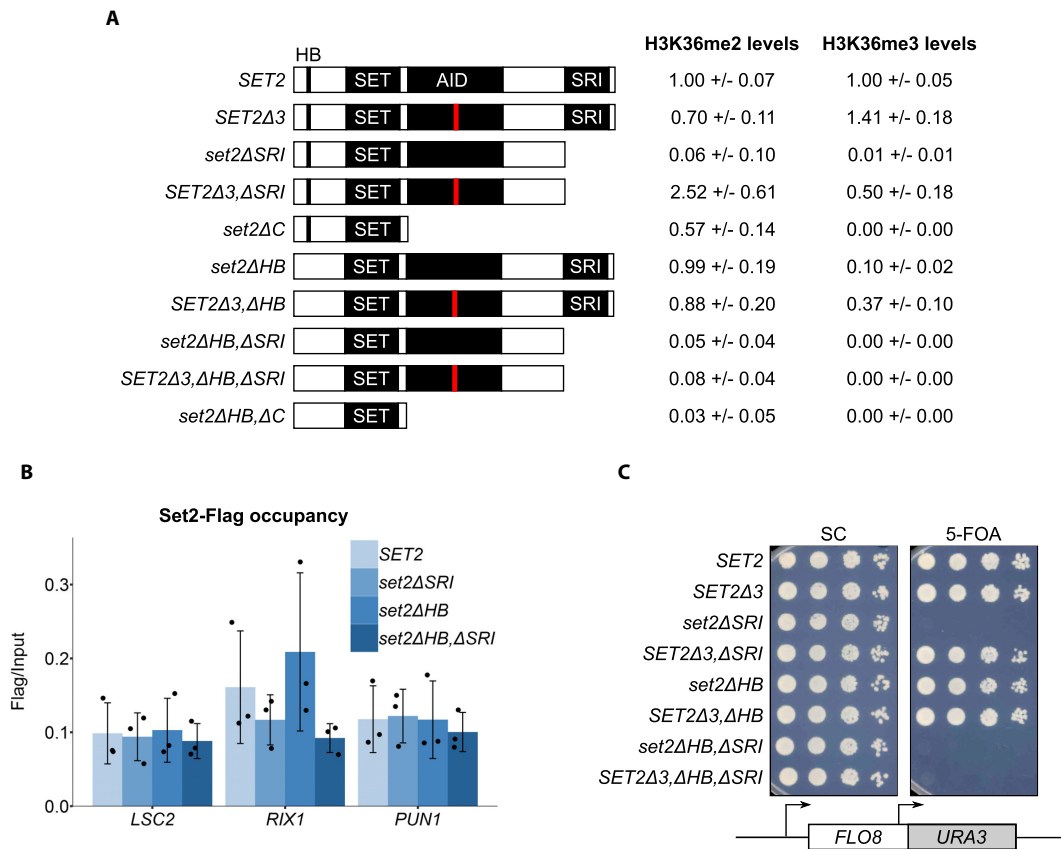
Figure 6. *SET2Δ3* rescues H3K36 methylation in *set2* mutants lacking the SRI or HB domains. (**A**) The schematic depicts Set2 and a set of mutants missing the indicated domains, testing each for H3K36me2 and H3K36me3 levels by western analysis. The red line in the AID represents the position of the *SET2Δ3* mutation. The numbers next to each mutation show the levels of H3K36me2 and H3K36me3 in each mutant strain relative to a wild-type control (mean ± standard deviation of at least three experiments). (**B**) ChIP-qPCR assaying localization of FLAG-tagged Set2 wild-type and mutant proteins at the *LSC2*, *RIX1* and *PUN1* genes. The black dots represent the individual data points for three experiments, and the bars show the mean ± standard deviation. ChIP-qPCR data have been spike-in normalized to the *Schizosaccharomyces pombe ACT1* gene. (**C**) Spot tests of cells grown at 37°C, assaying expression of the *FLO8-URA3* reporter in the indicated strains.

experiments were performed in four genetic backgrounds: wild type, *spt6-1004*, *spt6-1004 SET2-H366N* and *SET2-H366N*. Each condition was performed in duplicate and was highly reproducible (Supplementary Figure S4A). We chose *SET2-H366N* as it was the strongest suppressor of the *spt6-1004* H3K36me3 defect. To permit quantitative comparisons of ChIP signals between different samples, we used *S. pombe* chromatin for spike-in normalization ('Materials and methods' section and Supplementary Figure S4B).

Our results revealed new information regarding the H3K36 methylation defect caused by *spt6-1004* as well as the suppression of this defect by *SET2-H366N*. First, there was a large decrease genome-wide in *spt6-1004* in H3K36me2 and H3K36me3 association with chromatin as compared to the wild-type strain (Figure 7A and B), a result consistent with the observation that H3K36me2 and H3K36me3 are undetectable by westerns in *spt6-1004*. Second, in contrast to the large decrease in H3K36me2/me3, there was a little decrease in the level of Set2 protein recruited across transcribed regions when normalized to the level of Rpb1 (Figure 7C; Supplementary Figure S5A and B). Given these results, the defect in H3K36me2/me3 in the *spt6-1004* mutant must occur primarily at a level subsequent

to Set2 recruitment to chromatin. Third, in the *spt6-1004 SET2-H366N* double mutant, we saw a genome-wide rescue of H3K36me2/me3 (Figure 7A and B). Compared to the wild-type strain, this strain had generally increased levels of H3K36me2 and decreased levels of H3K36me3. Compared to the increase in histone methylation, Set2 localization to transcribed regions was only slightly increased as compared to *spt6-1004* (Figure 7C), showing that suppression by *SET2-H366N* was not due to increased recruitment to chromatin. Finally, the *SPT6 SET2-H366N* single mutant showed increased H3K36me3 and decreased H3K36me2 levels genome-wide as compared to wild-type (Figure 7A and B). However, in this strain the recruitment of Set2 to chromatin is modestly increased (Figure 7C), which may be due to the higher level of the Set2-H366N-Flag protein (Supplemental Figure S4C). No global changes in histone H3 occupancy were observed in any of the strains (Supplemental Figure S5C). ChIP-qPCR results at individual genes were consistent with our ChIP-seq results (see *STE11* and *RIX1*, Figure 7D-F; Supplemental Figure S5D-F). In summary, our results show that Spt6 is required for Set2 function after its recruitment to chromatin and suggest that this
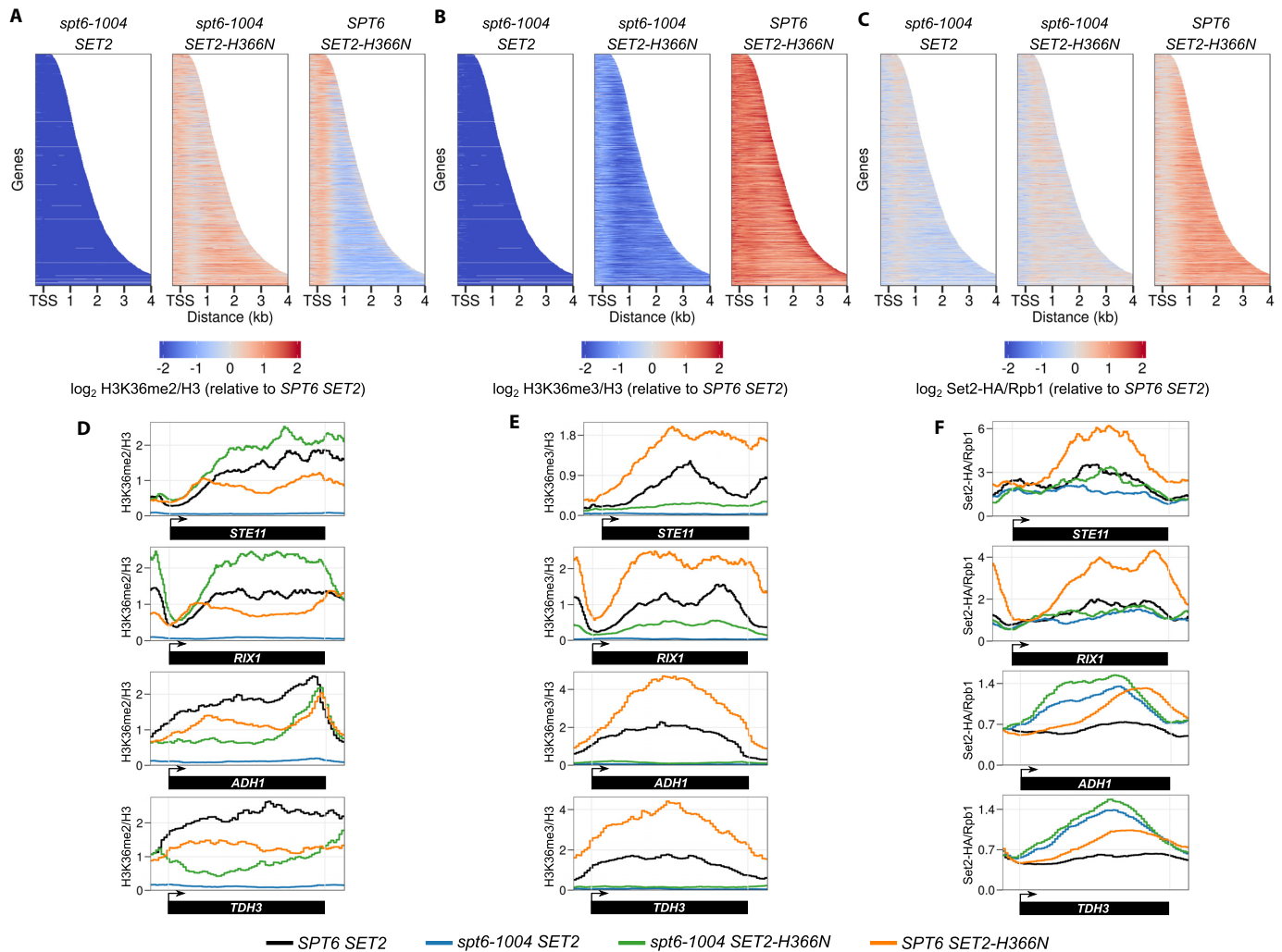
Figure 7. *SET2-H366N* rescues H3K36 methylation genome-wide in *spt6-1004*. (**A–C**) Heat maps depicting H3K36me2 levels (relative to H3) (A), H3K36me3 levels (relative to H3) (B) and Set2-HA levels (relative to Rpb1) (C) for all non-overlapping genes that code for protein (*n* = 3522). All values that had a log fold change of below −2 or above 2 have been set to −2 or 2, respectively. (**D-F**) H3K36me2 (D), H3K36me3 (E) and Set2-HA (F) levels at genes that show rescue of H3K36 methylation (*STE11*, *RIX1*) and genes where rescue of H3K36 methylation is not observed (*ADH1*, *TDH3*). All data have been normalized to an *S. pombe* spike-in control.

requirement is dependent upon the Set2 autoinhibitory domain.

Although the effects we observed occurred at most genes, a set of 48 genes behaved differently. In contrast to most genes, which had increased levels of H3K36me2 and partial rescue of H3K36me3 in the *spt6-1004 SET2-H366N* strains as compared to wild-type, this set of genes had reduced levels of H3K36me2 compared to wild-type. These genes had slightly decreased occupancy of histone H3 as compared to wild-type, but that decrease could not account for the decreased level of H3K36me2. In addition, Set2 recruitment was not impaired at these genes. Examples of two such genes, *ADH1* and *TDH3*, are shown in Figure 7D–F. GO term analysis indicated that these genes are enriched for those involved in ADP metabolic processes and cytoplasmic translation. To find out if this was a common trend among highly transcribed genes, we grouped genes by their expression level and determined H3K36me2/me3 levels in each of the groups. Our analysis revealed a slight decrease in H3K36me2/me3 levels in the most highly expressed genes relative to other groups in the *spt6-1004 SET2-H366N* strain (Supplementary Figure S5G). There appears to be some requirement for fully functional Set2 protein for H3K36 methylation at highly transcribed genes. However, this does not appear to be the sole determining characteristic among the set of 48 genes we have identified. Our results suggest the possibility of a different mechanism for regulation of Set2 activity at these genes.

The Set2–Spt6 genetic interaction is conserved

As both Set2 and Spt6 are conserved, including the Set2 autoinhibitory domain (Figure 8A) (49), we wanted to test whether the functional interactions between Set2 and Spt6 are conserved. To test this idea, we moved to *S. pombe*, a yeast that is as evolutionarily diverged from *S. cerevisiae* as either is from mammals (68). We constructed an *S. pombe* strain that contains a *set2* mutation similar to the *S. cere-*
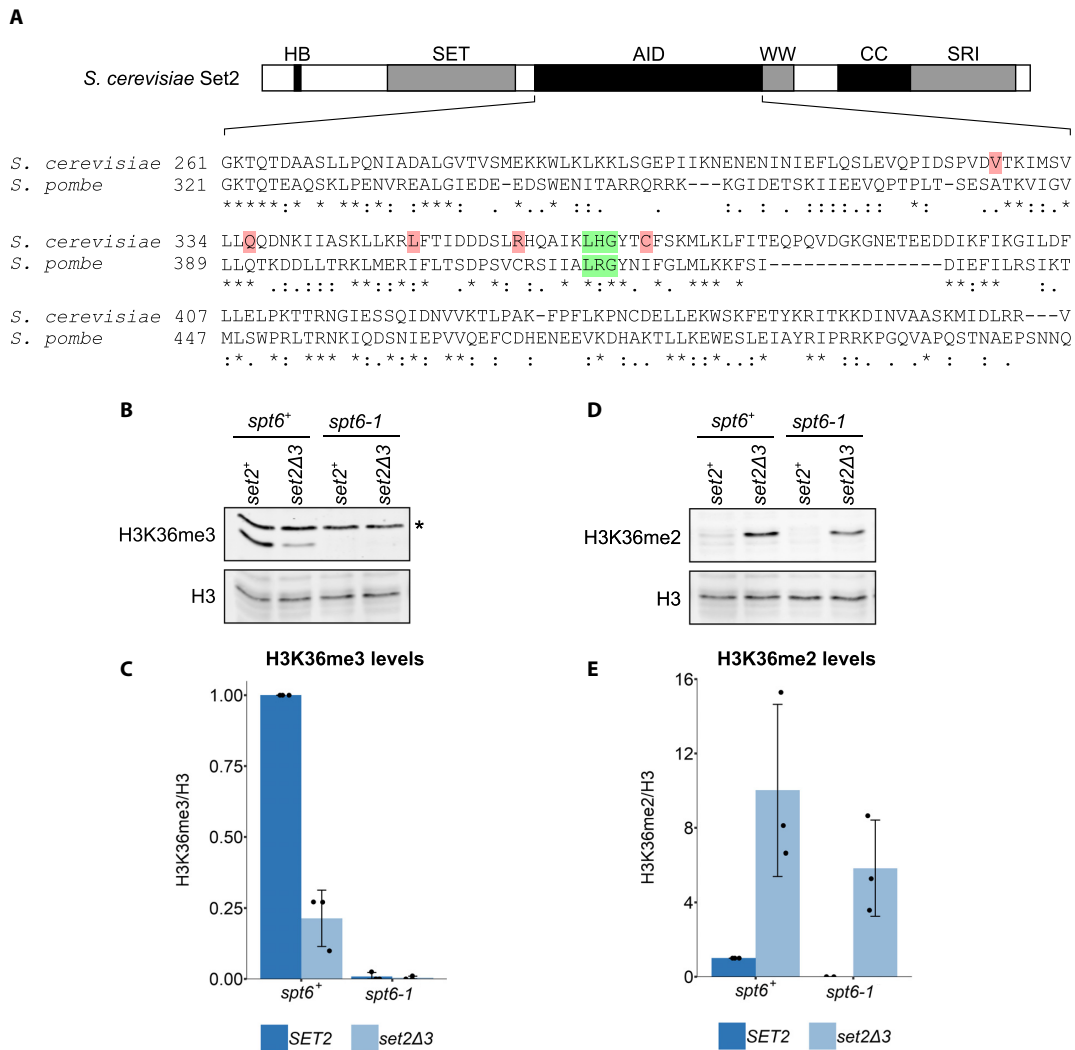
Figure 8. The genetic interaction between Spt6 and Set2 is conserved in *Schizosaccharomyces pombe*. (**A**) Conservation of the amino acid sequence of the central region of Set2 between *Saccharomyces cerevisiae* (amino acids 261–475) and *S. pombe*. The residues highlighted in green correspond to the three amino acids deleted in the *SET2Δ3* mutation. The residues highlighted in pink denote the location of the other *SET2^sup* mutations. An asterisk indicates an identical residue, a colon indicates a highly similar amino acid (scoring > 0.5 in the Gonnet PAM 250 matrix) and a period indicates a weakly similar amino acid (scoring ≤ 0.5 in the Gonnet PAM 250 matrix). (**B**) Western blot assaying the effect of the *set2Δ3* mutation on H3K36me3 levels in *spt6-1* cells in *S. pombe*. Histone H3 was used as a loading control. Asterisk denotes a non-specific band. (**C**) Quantification of western blots assaying H3K36me3 levels in the indicated strains. (**D**) Western blot assaying the effect of the *set2Δ3* mutation on H3K36me2 levels in *spt6-1* cells in *S. pombe*. Histone H3 was used as a loading control. (**E**) Quantification of western blots assaying H3K36me2 levels in the indicated strains. In both graphs, the black dots represent the individual data points for three experiments and the bars show the mean ± standard deviation.

visiae SET2Δ3 mutation (Figure 8A) and asked whether it could suppress the H3K36 methylation defect caused by an *S. pombe spt6* mutation. For these experiments, we used an *S. pombe spt6-1* mutant which, like *S. cerevisiae spt6-1004*, has a deletion of the sequence encoding the Spt6 HhH domain (24). This mutant has no detectable H3K36me2 or H3K36me3, while maintaining normal Set2 protein levels (24). Our results show that the *S. pombe set2Δ3* mutation suppressed the H3K36me2 defect in *spt6-1* although not the H3K36me3 defect (Figure 8B–E). The lack of suppression of the H3K36me3 defect is likely related to our finding that in a wild-type *spt6*⁺ background, the *S. pombe set2Δ3* mutation caused decreased levels H3K36me3 compared to wild-type, suggesting some functional differences for Set2 between the two species (69). In spite of these differences,

our results show that the autoinhibitory domain region of Set2 and its functional interaction with Spt6 is conserved between the two distantly related yeasts.

DISCUSSION

In this work we have presented new results about the regulation of Set2 activity in *S. cerevisiae,* providing insights into the requirements for Set2 to function during transcription elongation. By the isolation of *SET2^sup* mutations that partially suppress the requirement for Spt6 for H3K36 methylation, we have shown that a recently identified Set2 autoinhibitory domain (49) plays critical roles in the regulation of Set2 *in vivo*. Our results also suggest that the Set2 autoinhibitory domain dictates that Set2 will only be active in the

presence of Spt6 and the PAF complex. Furthermore, our results also suggest that the Set2 autoinhibitory domain requires that Set2 interacts with both RNAPII and histones via the Set2 SRI and HB domains, respectively, in order to function. We have demonstrated that the dependence of Set2 on Spt6 occurs genome-wide, at a step subsequent to the recruitment of Set2 to chromatin. Together, these results suggest a model in which the Set2 autoinhibitory domain evaluates multiple interactions between trans-acting factors and specific Set2 domains before allowing Set2 to catalyze H3K36me2/me3 *in vivo*. If any of the interactions fail to occur, then the Set2 autoinhibitory domain inhibits Set2 catalytic activity.

A majority of the single amino acid changes (18/20) identified by our *SET2^sup* mutations fall within a predicted single α helix of a proposed Set2 autoinhibitory domain (49). The tight clustering of our mutations likely reflects the stringency of our mutant selection. The nature of the mutations that we isolated suggests that they disrupt the α helix, thereby impairing the autoinhibitory domain, as seven of the 20 mutations encode proline. Furthermore, a deletion of the three codons that contained 13 of the 20 mutations also confers the same phenotype. The previous work that showed that deletion mutations spanning a four-helix region resulted in hyperactive Set2 proteins both *in vitro* and *in vivo*, although the *in vivo* analysis was limited by the instability of the mutant proteins (49). The *SET2^sup* mutations that we have isolated encode stable proteins, which allowed us to discover the critical role of the autoinhibitory domain *in vivo*.

Our results raise the question of the mechanism by which Spt6 is required for Set2 activity. At 30°C, the temperature at which our experiments were performed, the Spt6-1004 mutant protein is present at normal levels (25), yet there is no detectable H3K36me2/me3. The simplest possibility is that a direct interaction between the Spt6 HhH domain, the region missing in the Spt6-1004 mutant protein, and the Set2 autoinhibitory domain is required for Set2 activity. In support of this idea, the *spt6-1004* mutation causes the most severe defects in H3K36me2/me3 of all *spt6* alleles tested (18,67). However, there is no evidence for a direct Spt6–Set2 interaction, either by high-resolution analysis of Set2-interacting proteins (70) or by two-hybrid analysis (our unpublished results). We were also unable to detect any interaction between the autoinhibitory domain and other domains present in Set2 through co-immunoprecipitation and two-hybrid studies. While these negative results do not rule out a direct Set2–Spt6 interaction, it also seems plausible that in the *spt6-1004* mutant there is an altered chromatin configuration that impairs the interaction of Set2 with a nucleosomal surface post-recruitment, such as that previously identified to be required for Set2 activity (44,45).

Although the *SET2^sup* mutations are able to suppress the *spt6-1004* H3K36 methylation defect for most genes, there are a small number of genes at which H3K36 methylation is not rescued. This finding suggests that the mechanisms that regulate Set2 activity *in vivo* may not be uniform across the genome. The genes that behaved differently are highly transcribed and have a lower level of histone H3 compared to most genes; however, neither of those characteristics is sufficient to explain their lack of response to the *SET2^sup*

mutations. At these genes, there may be additional or distinct requirements for Set2 to function. Alternatively, these genes may recruit a high level of H3K36 demethylases or, as H3K36 can also be acetylated (71,72), these genes may be more subject to competition between these mutually exclusive modifications than at most other genes.

Autoinhibition is a common mode of regulation among histone methyltransferases in both yeast and mammals. For example, the *S. cerevisiae* H3K4 methyltransferase Set1 (73) and the *S. pombe* H3K9 methyltransferase Clr4 (74) both contain autoinhibitory domains. In addition, mammalian histone methyltransferases have been shown to contain autoinhibitory domains, including Nsd1 (75), PRDM9 (76) and Smyd3 (77). In these three cases, structural studies of the proteins have suggested likely mechanisms that are distinct from each other. There are at least two reasons that a methyltransferase such as Set2 would have such tight regulation of its activity. First, the requirement for interactions with both nucleosomes and elongating RNAPII, as well as the activities of factors such as Spt6 and Paf1, ensures that H3K36me2/me3 will only occur at the correct location and at the correct time—on chromatin when it is being actively transcribed. Second, this regulation provides the opportunity to regulate H3K36me2/me3 in different conditions. For example, recent studies have provided evidence that H3K36 methylation is important for nutrient stress response (32,78), carbon source shifts (79), DNA damage responses (80–83), splicing (84–87) and aging (88,89). Therefore, the Set2 autoinhibitory domain may serve as a target for additional regulators under particular growth conditions.

DATA AVAILABILITY

Genomic datasets are deposited in the Gene Expression Omnibus with accession number GSE116646. Other primary data are available from the corresponding author upon reasonable request.

SUPPLEMENTARY DATA

Supplementary Data are available at NAR Online.

REFERENCES

1. Close,D., Johnson,S.J., Sdano,M.A., McDonald,S.M., Robinson,H., Formosa,T. and Hill,C.P. (2011) Crystal structures of the S. cerevisiae Spt6 core and C-terminal tandem SH2 domain. *J. Mol. Biol.*, **408**, 697–713.
2. Diebold,M.L., Loeliger,E., Koch,M., Winston,F., Cavarelli,J. and Romier,C. (2010) Noncanonical tandem SH2 enables interaction of elongation factor Spt6 with RNA polymerase II. *J. Biol. Chem.*, **285**, 38389–38398.
3. Liu,J., Zhang,J., Gong,Q., Xiong,P., Huang,H., Wu,B., Lu,G., Wu,J. and Shi,Y. (2011) Solution structure of tandem SH2 domains from Spt6 protein and their binding to the phosphorylated RNA polymerase II C-terminal domain. *J. Biol. Chem.*, **286**, 29218–29226.
4. Sun,M., Lariviere,L., Dengl,S., Mayer,A. and Cramer,P. (2010) A tandem SH2 domain in transcription elongation factor Spt6 binds the phosphorylated RNA polymerase II C-terminal repeat domain (CTD). *J. Biol. Chem.*, **285**, 41597–41603.
5. Yoh,S.M., Cho,H., Pickle,L., Evans,R.M. and Jones,K.A. (2007) The Spt6 SH2 domain binds Ser2-P RNAPII to direct Iws1-dependent mRNA splicing and export. *Genes Dev.*, **21**, 160–174.
6. Sdano,M.A., Fulcher,J.M., Palani,S., Chandrasekharan,M.B., Parnell,T.J., Whitby,F.G., Formosa,T. and Hill,C.P. (2017) A novel SH2 recognition mechanism recruits Spt6 to the doubly phosphorylated RNA polymerase II linker at sites of transcription. *Elife*, **6**, e28723.
7. McCullough,L., Connell,Z., Petersen,C. and Formosa,T. (2015) The abundant histone chaperones Spt6 and FACT collaborate to assemble, inspect, and maintain chromatin structure in saccharomyces cerevisiae. *Genetics*, **201**, 1031–1045.
8. Bortvin,A. and Winston,F. (1996) Evidence that Spt6p controls chromatin structure by a direct interaction with histones. *Science*, **272**, 1473–1476.
9. McDonald,S.M., Close,D., Xin,H., Formosa,T. and Hill,C.P. (2010) Structure and biological importance of the Spn1-Spt6 interaction, and its regulatory role in nucleosome binding. *Mol. Cell*, **40**, 725–735.
10. Diebold,M.L., Koch,M., Loeliger,E., Cura,V., Winston,F., Cavarelli,J. and Romier,C. (2010) The structure of an Iws1/Spt6 complex reveals an interaction domain conserved in TFIIS, Elongin A and Med26. *EMBO J.*, **29**, 3979–3991.
11. Krogan,N.J., Kim,M., Ahn,S.H., Zhong,G., Kobor,M.S., Cagney,G., Emili,A., Shilatifard,A., Buratowski,S. and Greenblatt,J.F. (2002) RNA polymerase II elongation factors of Saccharomyces cerevisiae: a targeted proteomics approach. *Mol. Cell. Biol.*, **22**, 6979–6992.
12. Lindstrom,D.L., Squazzo,S.L., Muster,N., Burckin,T.A., Wachter,K.C., Emigh,C.A., McCleery,J.A., Yates,J.R. 3rd and Hartzog,G.A. (2003) Dual roles for Spt5 in pre-mRNA processing and transcription elongation revealed by identification of Spt5-associated proteins. *Mol. Cell. Biol.*, **23**, 1368–1378.
13. Perales,R., Erickson,B., Zhang,L., Kim,H., Valiquett,E. and Bentley,D. (2013) Gene promoters dictate histone occupancy within genes. *EMBO J.*, **32**, 2645–2656.
14. Ivanovska,I., Jacques,P.E., Rando,O.J., Robert,F. and Winston,F. (2011) Control of chromatin structure by spt6: different consequences in coding and regulatory regions. *Mol. Cell. Biol.*, **31**, 531–541.
15. van Bakel,H., Tsui,K., Gebbia,M., Mnaimneh,S., Hughes,T.R. and Nislow,C. (2013) A compendium of nucleosome and transcript profiles reveals determinants of chromatin architecture and transcription. *PLos Genet.*, **9**, e1003479.
16. Jeronimo,C., Watanabe,S., Kaplan,C.D., Peterson,C.L. and Robert,F. (2015) The histone chaperones FACT and Spt6 restrict H2A.Z from intragenic locations. *Mol. Cell*, **58**, 1113–1123.
17. Carrozza,M.J., Li,B., Florens,L., Suganuma,T., Swanson,S.K., Lee,K.K., Shia,W.J., Anderson,S., Yates,J., Washburn,M.P. *et al.* (2005) Histone H3 methylation by Set2 directs deacetylation of coding regions by Rpd3S to suppress spurious intragenic transcription. *Cell*, **123**, 581–592.
18. Chu,Y., Sutton,A., Sternglanz,R. and Prelich,G. (2006) The BUR1 cyclin-dependent protein kinase is required for the normal pattern of histone methylation by SET2. *Mol. Cell. Biol.*, **26**, 3029–3038.
19. Youdell,M.L., Kizer,K.O., Kisseleva-Romanova,E., Fuchs,S.M., Duro,E., Strahl,B.D. and Mellor,J. (2008) Roles for Ctk1 and Spt6 in regulating the different methylation states of histone H3 lysine 36. *Mol. Cell. Biol.*, **28**, 4915–4926.
20. Strahl,B.D., Grant,P.A., Briggs,S.D., Sun,Z.W., Bone,J.R., Caldwell,J.A., Mollah,S., Cook,R.G., Shabanowitz,J., Hunt,D.F. *et al.* (2002) Set2 is a nucleosomal histone H3-selective methyltransferase that mediates transcriptional repression. *Mol. Cell Biol.*, **22**, 1298–1306.
21. Kaplan,C.D., Laprade,L. and Winston,F. (2003) Transcription elongation factors repress transcription initiation from cryptic sites. *Science*, **301**, 1096–1099.
22. Cheung,V., Chua,G., Batada,N.N., Landry,C.R., Michnick,S.W., Hughes,T.R. and Winston,F. (2008) Chromatin- and transcription-related factors repress transcription from within coding regions throughout the Saccharomyces cerevisiae genome. *PLoS Biol.*, **6**, e277.
23. Uwimana,N., Collin,P., Jeronimo,C., Haibe-Kains,B. and Robert,F. (2017) Bidirectional terminators in Saccharomyces cerevisiae prevent cryptic transcription from invading neighboring genes. *Nucleic Acids Res.*, **45**, 6417–6426.
24. DeGennaro,C.M., Alver,B.H., Marguerat,S., Stepanova,E., Davis,C.P., Bahler,J., Park,P.J. and Winston,F. (2013) Spt6 regulates intragenic and antisense transcription, nucleosome positioning, and histone modifications genome-wide in fission yeast. *Mol. Cell Biol.*, **33**, 4779–4792.
25. Doris,S.M., Chuang,J., Viktorovskaya,O., Murawska, M., Spatt, D., Churchman, L.S. and Winston,F. (2018) Spt6 is required for the fidelity of promoter selection. *Mol. Cell*, **72**, 687–699.
26. Gammie,A.E., Stewart,B.G., Scott,C.F. and Rose,M.D. (1999) The two forms of karyogamy transcription factor Kar4p are regulated by differential initiation of transcription, translation, and protein turnover. *Mol. Cell Biol.*, **19**, 817–825.
27. McKnight,K., Liu,H. and Wang,Y. (2014) Replicative stress induces intragenic transcription of the ASE1 gene that negatively regulates Ase1 activity. *Curr. Biol.*, **24**, 1101–1106.
28. Zhou,S., Sternglanz,R. and Neiman,A.M. (2017) Developmentally regulated internal transcription initiation during meiosis in budding yeast. *PLoS One*, **12**, e0188001.
29. Tamarkin-Ben-Harush,A., Vasseur,J.J., Debart,F., Ulitsky,I. and Dikstein,R. (2017) Cap-proximal nucleotides via differential eIF4E binding and alternative promoter usage mediate translational response to energy stress. *Elife*, **6**, e21907.
30. Ushijima,T., Hanada,K., Gotoh,E., Yamori,W., Kodama,Y., Tanaka,H., Kusano,M., Fukushima,A., Tokizawa,M., Yamamoto,Y.Y. *et al.* (2017) Light Controls Protein Localization through Phytochrome-Mediated Alternative Promoter Selection. *Cell*, **171**, 1316–1325.
31. Li,B., Gogol,M., Carey,M., Pattenden,S.G., Seidel,C. and Workman,J.L. (2007) Infrequently transcribed long genes depend on the Set2/Rpd3S pathway for accurate transcription. *Genes Dev.*, **21**, 1422–1430.
32. Venkatesh,S., Li,H., Gogol,M.M. and Workman,J.L. (2016) Selective suppression of antisense transcription by Set2-mediated H3K36 methylation. *Nat. Commun.*, **7**, 13610.
33. Krogan,N.J., Kim,M., Tong,A., Golshani,A., Cagney,G., Canadien,V., Richards,D.P., Beattie,B.K., Emili,A., Boone,C. *et al.* (2003) Methylation of histone H3 by Set2 in Saccharomyces cerevisiae is linked to transcriptional elongation by RNA polymerase II. *Mol. Cell. Biol.*, **23**, 4207–4218.
34. Li,B., Howe,L., Anderson,S., Yates,J.R. and Workman,J.L. (2003) The Set2 histone methyltransferase functions through the phosphorylated carboxyl-terminal domain of RNA polymerase II. *J. Biol. Chem.*, **278**, 8897–8903.
35. Li,J., Moazed,D. and Gygi,S.P. (2002) Association of the histone methyltransferase Set2 with RNA polymerase II plays a role in transcription elongation. *J. Biol. Chem.*, **277**, 49383–49388.
36. Xiao,T., Hall,H., Kizer,K.O., Shibata,Y., Hall,M.C., Borchers,C.H. and Strahl,B.D. (2003) Phosphorylation of RNA polymerase II CTD regulates H3 methylation in yeast. *Genes Dev.*, **17**, 654–663.
37. Drouin,S., Laramee,L., Jacques,P.E., Forest,A., Bergeron,M. and Robert,F. (2010) DSIF and RNA polymerase II CTD phosphorylation coordinate the recruitment of Rpd3S to actively transcribed genes. *PLos Genet.*, **6**, e1001173.
38. Govind,C.K., Qiu,H., Ginsburg,D.S., Ruan,C., Hofmeyer,K., Hu,C., Swaminathan,V., Workman,J.L., Li,B. and Hinnebusch,A.G. (2010) Phosphorylated Pol II CTD recruits multiple HDACs, including

Rpd3C(S), for methylation-dependent deacetylation of ORF nucleosomes. *Mol. Cell*, **39**, 234–246.

39. Joshi,A.A. and Struhl,K. (2005) Eaf3 chromodomain interaction with methylated H3-K36 links histone deacetylation to Pol II elongation. *Mol. Cell*, **20**, 971–978.

40. Keogh,M.C., Kurdistani,S.K., Morris,S.A., Ahn,S.H., Podolny,V., Collins,S.R., Schuldiner,M., Chin,K., Punna,T., Thompson,N.J. *et al.* (2005) Cotranscriptional set2 methylation of histone H3 lysine 36 recruits a repressive Rpd3 complex. *Cell*, **123**, 593–605.

41. Carvalho,S., Raposo,A.C., Martins,F.B., Grosso,A.R., Sridhara,S.C., Rino,J., Carmo-Fonseca,M. and de Almeida,S.F. (2013) Histone methyltransferase SETD2 coordinates FACT recruitment with nucleosome dynamics during transcription. *Nucleic Acids Res.*, **41**, 2881–2893.

42. Chu,Y., Simic,R., Warner,M.H., Arndt,K.M. and Prelich,G. (2007) Regulation of histone modification and cryptic transcription by the Bur1 and Paf1 complexes. *EMBO J.*, **26**, 4646–4656.

43. Fuchs,S.M., Kizer,K.O., Braberg,H., Krogan,N.J. and Strahl,B.D. (2012) RNA polymerase II carboxyl-terminal domain phosphorylation regulates protein stability of the Set2 methyltransferase and histone H3 di- and trimethylation at lysine 36. *J. Biol. Chem.*, **287**, 3249–3256.

44. Du,H.N. and Briggs,S.D. (2010) A nucleosome surface formed by histone H4, H2A, and H3 residues is needed for proper histone H3 Lys36 methylation, histone acetylation, and repression of cryptic transcription. *J. Biol. Chem.*, **285**, 11704–11713.

45. Du,H.N., Fingerman,I.M. and Briggs,S.D. (2008) Histone H3 K36 methylation is mediated by a trans-histone methylation pathway involving an interaction between Set2 and histone H4. *Genes Dev.*, **22**, 2786–2798.

46. Psathas,J.N., Zheng,S., Tan,S. and Reese,J.C. (2009) Set2-dependent K36 methylation is regulated by novel intratail interactions within H3. *Mol. Cell Biol.*, **29**, 6413–6426.

47. Nelson,C.J., Santos-Rosa,H. and Kouzarides,T. (2006) Proline isomerization of histone H3 regulates lysine methylation and gene expression. *Cell*, **126**, 905–916.

48. Kizer,K.O., Phatnani,H.P., Shibata,Y., Hall,H., Greenleaf,A.L. and Strahl,B.D. (2005) A novel domain in Set2 mediates RNA polymerase II interaction and couples histone H3 K36 methylation with transcript elongation. *Mol. Cell Biol.*, **25**, 3305–3316.

49. Wang,Y., Niu,Y. and Li,B. (2015) Balancing acts of SRI and an auto-inhibitory domain specify Set2 function at transcribed chromatin. *Nucleic Acids Res.*, **43**, 4881–4892.

50. Ruan,C., Lee,C.H., Cui,H., Li,S. and Li,B. (2015) Nucleosome contact triggers conformational changes of Rpd3S driving high-affinity H3K36me nucleosome engagement. *Cell Rep.*, **10**, 204–215.

51. Longtine,M.S., McKenzie,A. 3rd, Demarini,D.J., Shah,N.G., Wach,A., Brachat,A., Philippsen,P. and Pringle,J.R. (1998) Additional modules for versatile and economical PCR-based gene deletion and modification in Saccharomyces cerevisiae. *Yeast*, **14**, 953–961.

52. Ghaemmaghami,S., Huh,W.K., Bower,K., Howson,R.W., Belle,A., Dephoure,N., O'Shea,E.K. and Weissman,J.S. (2003) Global analysis of protein expression in yeast. *Nature*, **425**, 737–741.

53. Storici,F. and Resnick,M.A. (2006) The delitto perfetto approach to in vivo site-directed mutagenesis and chromosome rearrangements with synthetic oligonucleotides in yeast. *Methods Enzymol.*, **409**, 329–345.

54. Wong,K.H., Jin,Y. and Moqtaderi,Z. (2013) Multiplex Illumina sequencing using DNA barcoding. *Curr. Protoc. Mol. Biol.*, doi:10.1002/0471142727.mb0711s101.

55. Langmead,B. and Salzberg,S.L. (2012) Fast gapped-read alignment with Bowtie 2. *Nat. Methods*, **9**, 357–359.

56. Li,H., Handsaker,B., Wysoker,A., Fennell,T., Ruan,J., Homer,N., Marth,G., Abecasis,G., Durbin,R. and Genome Project Data Processing, S. (2009) The sequence alignment/Map format and SAMtools. *Bioinformatics*, **25**, 2078–2079.

57. Matsuo,Y., Asakawa,K., Toda,T. and Katayama,S. (2006) A rapid method for protein extraction from fission yeast. *Biosci. Biotechnol. Biochem.*, **70**, 1992–1994.

58. Ausubel,F.M., Brent,R., Kingston,R.E., Moore,D.D., Seidman,J.G., Smith,J.A. and Struhl,K. (eds). (1991) *Current Protocols in Molecular Biology*. Greene Publishing Associates and Wiley-Interscience, NY.

59. Gibson,D.G., Young,L., Chuang,R.Y., Venter,J.C., Hutchison,C.A. 3rd and Smith,H.O. (2009) Enzymatic assembly of DNA molecules up to several hundred kilobases. *Nat. Methods*, **6**, 343–345.

60. Bradford,M.M. (1976) A rapid and sensitive method for the quantitation of microgram quantities of protein utilizing the principle of protein-dye binding. *Anal. Biochem.*, **72**, 248–254.

61. Koster,J. and Rahmann,S. (2012) Snakemake–a scalable bioinformatics workflow engine. *Bioinformatics*, **28**, 2520–2522.

62. Kharchenko,P.V., Tolstorukov,M.Y. and Park,P.J. (2008) Design and analysis of ChIP-seq experiments for DNA-binding proteins. *Nat. Biotechnol.*, **26**, 1351–1359.

63. Thorvaldsdottir,H., Robinson,J.T. and Mesirov,J.P. (2013) Integrative Genomics Viewer (IGV): high-performance genomics data visualization and exploration. *Brief. Bioinform.*, **14**, 178–192.

64. Orlando,D.A., Chen,M.W., Brown,V.E., Solanki,S., Choi,Y.J., Olson,E.R., Fritz,C.C., Bradner,J.E. and Guenther,M.G. (2014) Quantitative ChIP-Seq normalization reveals global modulation of the epigenome. *Cell Rep.*, **9**, 1163–1170.

65. Quinlan,A.R. and Hall,I.M. (2010) BEDTools: a flexible suite of utilities for comparing genomic features. *Bioinformatics*, **26**, 841–842.

66. Nishimura,K., Fukagawa,T., Takisawa,H., Kakimoto,T. and Kanemaki,M. (2009) An auxin-based degron system for the rapid depletion of proteins in nonplant cells. *Nat. Methods*, **6**, 917–922.

67. Dronamraju,R. and Strahl,B.D. (2014) A feed forward circuit comprising Spt6, Ctk1 and PAF regulates Pol II CTD phosphorylation and transcription elongation. *Nucleic Acids Res.*, **42**, 870–881.

68. Sipiczki,M. (2000) Where does fission yeast sit on the tree of life? *Genome Biol.*, **1**, REVIEWS1011.

69. Suzuki,S., Kato,H., Suzuki,Y., Chikashige,Y., Hiraoka,Y., Kimura,H., Nagao,K., Obuse,C., Takahata,S. and Murakami,Y. (2016) Histone H3K36 trimethylation is essential for multiple silencing mechanisms in fission yeast. *Nucleic Acids Res.*, **44**, 4147–4162.

70. Mosley,A.L., Hunter,G.O., Sardiu,M.E., Smolle,M., Workman,J.L., Florens,L. and Washburn,M.P. (2013) Quantitative proteomics demonstrates that the RNA polymerase II subunits Rpb4 and Rpb7 dissociate during transcriptional elongation. *Mol. Cell Proteomics*, **12**, 1530–1538.

71. Ngubo,M., Kemp,G. and Patterton,H.G. (2011) Nano-electrospray tandem mass spectrometric analysis of the acetylation state of histones H3 and H4 in stationary phase in Saccharomyces cerevisiae. *BMC Biochem.*, **12**, 34.

72. Tang,H., Fang,H., Yin,E., Brasier,A.R., Sowers,L.C. and Zhang,K. (2014) Multiplexed parallel reaction monitoring targeting histone modifications on the QExactive mass spectrometer. *Anal. Chem.*, **86**, 5526–5534.

73. Schlichter,A. and Cairns,B.R. (2005) Histone trimethylation by Set1 is coordinated by the RRM, autoinhibitory, and catalytic domains. *EMBO J.*, **24**, 1222–1231.

74. Iglesias,N., Currie,M.A., Jih,G., Paulo,J.A. *et al.* (2018) Automethylation-induced conformational switch in Clr4 (Suv39h) maintains epigenetic stability. *Nature*, **560**, 504–508.

75. Qiao,Q., Li,Y., Chen,Z., Wang,M., Reinberg,D. and Xu,R.M. (2011) The structure of NSD1 reveals an autoregulatory mechanism underlying histone H3K36 methylation. *J. Biol. Chem.*, **286**, 8361–8368.

76. Wu,H., Mathioudakis,N., Diagouraga,B., Dong,A., Dombrovski,L., Baudat,F., Cusack,S., de Massy,B. and Kadlec,J. (2013) Molecular basis for the regulation of the H3K4 methyltransferase activity of PRDM9. *Cell Rep.*, **5**, 13–20.

77. Sirinupong,N., Brunzelle,J., Doko,E. and Yang,Z. (2011) Structural insights into the autoinhibition and posttranslational activation of histone methyltransferase SmyD3. *J. Mol. Biol.*, **406**, 149–159.

78. McDaniel,S.L., Hepperla,A.J., Huang,J., Dronamraju,R., Adams,A.T., Kulkarni,V.G., Davis,I.J. and Strahl,B.D. (2017) H3K36 methylation regulates nutrient stress response in saccharomyces cerevisiae by enforcing transcriptional fidelity. *Cell Rep.*, **19**, 2371–2382.

79. Kim,J.H., Lee,B.B., Oh,Y.M., Zhu,C., Steinmetz,L.M., Lee,Y., Kim,W.K., Lee,S.B., Buratowski,S. and Kim,T. (2016) Modulation of mRNA and lncRNA expression dynamics by the Set2-Rpd3S pathway. *Nat. Commun.*, **7**, 13534.

80. Carvalho,S., Vitor,A.C., Sridhara,S.C., Martins,F.B., Raposo,A.C., Desterro,J.M., Ferreira,J. and de Almeida,S.F. (2014) SETD2 is required for DNA double-strand break repair and activation of the p53-mediated checkpoint. *Elife*, **3**, e02482.

81. Jha,D.K. and Strahl,B.D. (2014) An RNA polymerase II-coupled function for histone H3K36 methylation in checkpoint activation and DSB repair. *Nat. Commun.*, **5**, 3965.

82. Li,F., Mao,G., Tong,D., Huang,J., Gu,L., Yang,W. and Li,G.M. (2013) The histone mark H3K36me3 regulates human DNA mismatch repair through its interaction with MutSalpha. *Cell*, **153**, 590–600.

83. Pfister,S.X., Markkanen,E., Jiang,Y., Sarkar,S., Woodcock,M., Orlando,G., Mavrommati,I., Pai,C.C., Zalmas,L.P., Drobnitzky,N. *et al.* (2015) Inhibiting WEE1 selectively kills histone H3K36me3-Deficient cancers by dNTP starvation. *Cancer Cell*, **28**, 557–568.

84. Luco,R.F., Pan,Q., Tominaga,K., Blencowe,B.J., Pereira-Smith,O.M. and Misteli,T. (2010) Regulation of alternative splicing by histone modifications. *Science*, **327**, 996–1000.

85. Sanidas,I., Polytarchou,C., Hatziapostolou,M., Ezell,S.A., Kottakis,F., Hu,L., Guo,A., Xie,J., Comb,M.J., Iliopoulos,D. *et al.* (2014) Phosphoproteomics screen reveals akt isoform-specific signals linking RNA processing to lung cancer. *Mol. Cell*, **53**, 577–590.

86. Sorenson,M.R., Jha,D.K., Ucles,S.A., Flood,D.M., Strahl,B.D., Stevens,S.W. and Kress,T.L. (2016) Histone H3K36 methylation regulates pre-mRNA splicing in Saccharomyces cerevisiae. *RNA Biol.*, **13**, 412–426.

87. Yuan,H., Li,N., Fu,D., Ren,J., Hui,J., Peng,J., Liu,Y., Qiu,T., Jiang,M., Pan,Q. *et al.* (2017) Histone methyltransferase SETD2 modulates alternative splicing to inhibit intestinal tumorigenesis. *J. Clin. Invest.*, **127**, 3375–3391.

88. Ryu,H.Y., Rhie,B.H. and Ahn,S.H. (2014) Loss of the Set2 histone methyltransferase increases cellular lifespan in yeast cells. *Biochem. Biophys. Res. Commun.*, **446**, 113–118.

89. Sen,P., Dang,W., Donahue,G., Dai,J., Dorsey,J., Cao,X., Liu,W., Cao,K., Perry,R., Lee,J.Y. *et al.* (2015) H3K36 methylation promotes longevity by enhancing transcriptional fidelity. *Genes Dev.*, **29**, 1362–1376.